IEEE Access
Multidisciplinary ⋮ Rapid Review ⋮ Open Access Journal

Received 15 January 2024, accepted 26 January 2024, date of publication 30 January 2024, date of current version 7 February 2024.

Digital Object Identifier 10.1109/ACCESS.2024.3360132

RESEARCH ARTICLE

Parameterization of Circuit Breakers for HVDC Transmission Line Between Egypt and the Kingdom of Saudi Arabia Toward Restriking Voltage

TAMER ELIYAN[1,2], MAHMOUD ELSISI[1,3], (Senior Member, IEEE), MAMDOUH L. ALGHAYTHI[4], (Member, IEEE), MESHARI S. ALSHAMMARI[4], AND FADY WADIE[5]

[1]Department of Electrical Engineering, Faculty of Engineering at Shoubra, Benha University, Cairo 11629, Egypt
[2]Department of Electrical Power & Machines Engineering, Higher Institute of Engineering at El-Shorouk City, Alshorouk Academy, Cairo 11837, Egypt
[3]Department of Electrical Engineering, National Kaohsiung University of Science and Technology, Kaohsiung 807618, Taiwan
[4]Department of Electrical Engineering, College of Engineering, Jouf University, Sakaka 72388, Saudi Arabia
[5]Mechatronics and Robotics Engineering Department, Faculty of Engineering, Egyptian Russian University, Badr City 11829, Egypt

Corresponding authors: Tamer Eliyan (tamer.alyan@feng.bu.edu.eg) and Mahmoud Elsisi (mahmoud.elsesy@feng.bu.edu.eg; mahmoudelsisi@nkust.edu.tw)

This work was supported by the Deputyship for Research and Innovation, Ministry of Education in Saudi Arabia, under Project 223202.

ABSTRACT The high voltage direct current (HVDC) transmission lines represent the prospective way for long-distance transmission between countries, remote areas, and offshore wind farms to decrease power loss. However, the HVDC protection systems have many challenges against any system issue, such as maintenance and short circuits. Thus, the vital role played by high voltage direct current circuit breaker CB has made it the center of attention in HVDC protection systems. The main challenge in HVDC CB is the lack of naturally exiting current zero that allows the breaker to extinguish the arc during the opening process. Thus, a commutation L-C circuit is required to inject an oscillating current and enforce a zero-crossing. Nevertheless, the L-C branch is affected directly by the arcing time, the transient recovery voltage (TRV), and the rate of rise of recovery voltage (RRRV). This paper investigates the parametric uncertainties of L-C and SF6 mechanical interrupters, including cooling power and arc time constant upon TRV and RRRV, based on Mayr's black-box model. Furthermore, a part of 3000 MVA, 500 kV HVDC transmission line between Egypt and the Kingdom of Saudi Arabia is used as a testing system employing ATP/EMTP software package to demonstrate the effect of CB's parameters variations. The results indicate that the capacitance represents the major parameter having a direct impact on TRV and RRRV. In essence, the proper parameterization of the CB is highly required in the design process of HVDC CB to enhance the decision-making and ensure that the L-C is capable of reducing arcing time and TRV simultaneously.

INDEX TERMS Transmission lines, HVDC, protection systems, circuit breakers, TRV, RRRV, black-box arc model, arcing time.

NOMENCLATURE

ACSR/AW	: Aluminum-Clad Steel Reinforced/ American Wire.
CB	: Circuit breaker.
g_m	: Conductance of the arc.
HVDC	: High voltage direct current.
MOV	: Metal–oxide varistor.
P_H	: Heating power of arc.
P_o	: Cooling power.
Q	: Energy stored in the arc.
RRRV	: Rate of rise of recovery voltage.

The associate editor coordinating the review of this manuscript and approving it for publication was Ali Raza.

τ : Arc time constant.
TRV : Transient recovery voltage.

I. INTRODUCTION

Evolving power systems to become globally extending across wide geographical space have pushed the growth of high voltage direct current (HVDC) transmission [1], [2], [3]. This interest is attributed to the superiority of HVDC systems in transmitting bulk power through long distances and interconnecting unsynchronized power systems [4], [5], [6], [7]. That increased reliance on HVDC transmission was reflected upon HVDC protection systems with a specific focus on HVDC circuit breakers (CB) and their arc interruption technologies [8], [9]. HVDC CB's main challenge is the need for naturally commutated current zero crossing. That mandated a forced current zero commutation device to be incorporated within the HVDC CB topology [10], [11]. Therefore, the topology of HVDC CB is manufactured of an interrupting element, either gaseous or vacuum, and a parallel resonant L-C filter-branch to generate artificial zero crossing to allow arc interruption [12], [13], [14]. Two additional parallel components are also used, an R-C component and a metal–oxide varistor (MOV). The R-C branch is used to control the rate of rise of recovery voltage (RRRV), while the MOV is used to absorb the excess energy following the arc interruption process [15], [16], [17], [18].

The modeling of the interrupting element is dependent on its type of arc vanquishing technology, either employing a vacuum or SF6 interrupter [19], [20], [21], [22]. The modeling of the SF6 arc extinguishing process is available in literature as physical or black box arc models. The physical model is highly detailed in defining the arc interruption process, making it complex in application. At the same time, the black box model deals with the variation of the non-linear arc conductance [23], [24], [25], [26]. Cassie and Mayr dynamic arc equations are the most widely used in the black box model [15], [16], [17]. That filter is only used with Mayr's model, while Cassie's model only requires steady-state arc voltage over supply voltage to decrease current to zero [14]. The Mayr model will be used in modeling the SF6 interrupter in this paper in HVDC CB.

The parallel branches, including L-C commutation filter and energy-absorbing elements, have been widely investigated in literature to optimize their arcing quenching capability [12], [13], [14], [27], [28], [29], [30], [31], [32]. Supercapacitors (SCs) are characterized by their high capacitance and time constants from fractional seconds to seconds. Due to these relatively long-time constants compared to the fast transients in power systems, these devices may be able to withstand short-duration surges [33], [34], [35]. Table 1 provides a summary of the literature on this topic.

The impact of different parameters of different topologies were also investigated in literature [36], [37], [38], [39]. The effect of changing parameters with hybrid circuit breaker topology combining mechanical and solid state switches were investigated in [36]. A natural commutation current topology used for hybrid HVDC was combined with fault current limiter in [37]. The impact of such topology upon fault current rising slope was studied [37]. Also, a proposed reactor based hybrid DC circuit breaker had shown to reduce the rising rate and peak of the fault current [39]. It could be shown that the impact of changing parameters of hybrid topology circuit breaker is relatively close in its manner when compared to mechanical HVDC circuit breaker.

Most of the previous literature focused on the arch quenching capability of the circuit breaker, leaving the transient recovery voltage (TRV) and the rate of rise of recovery voltage (RRRV) un-tackled. Therefore, the main problem that this paper focuses on is addressing the gap in the literature regarding the impact of the parameters of CB upon TRV and RRRV. Hence, in this paper, the effect of variation of their parameters on the performance of the CB upon the TRV and RRRV will be studied. These parameters include the L-C filter, the power cooling, and the arc time constant of the interrupter. The main contribution of the paper could be summarized as follows: Investigating the effect of the Mayr model parameters upon the TRV and RRRV arising after the interruption of the arc; Investigating the effect of the L-C filter parameters upon the

TABLE 1. Summary of literatre.

Topics Studied	12	13	14	27	29	31	32	33
Effect of parameters on arcing time using cascaded black box model	-	✓	-	-	-	-	-	-
Effect of superconducting element on arcing time	✓	-	-	✓	-	-	-	-
Effect of Additional elements upon element on performance of HVDC CB	✓	-	-	✓	✓	✓	-	-
Effect of Commutation circuit upon element on arcing time	-	-	✓	-	-	-	✓	-
Effect of supercapacitors on arcing time	✓	-	-	-	-	-	-	✓

TRV and RRRV. Simulation software are going to be used as it was considered a reliable research methodology by earlier research community [12], [13], [14], [15], [16], [27], [28], [29], [30], [31], [32], [33] and their results proved to be in agreement with experimental results [29].

The rest of this paper is organized as follows. Section II presents the modeling of the SF6 current interrupter using Mayr model. The breaker was used in protecting a real transmission line in Egypt using ATP/EMTP software and the results of the simulation for the effect of the parameters' variations of various interrupter models upon TRV and RRRV are presented in section III. In section IV, the impact of CB parameters upon TRV and RRRV is discussed. Finally, conclusions are drawn in section V.

II. MODELING OF THE HVDC CIRCUIT BREAKER

A. MODELING OF THE SF6 INTERRUPTER

The circuit breaker used has a topology of mechanical HVDC circuit breaker with SF6 interrupter used. The SF6 interrupter is modeled using Mayr's black-box model. Other models include Browne model. The Browne model is based on the assumption that during the critical period, the current can be represented by a linearly decreasing ramp function, until the current zero [40], [41], [42]. On this paper Mayr's model is used. Mayr's model is characterized by its ability to execute dynamic analysis for the arc to define the capability of the breaker to interrupt the arc [12]. Such dynamic analysis allows Mayr arc model to be suitable for arc interruption in gases. The mathematical formulation of the model is done through the calculation of the variable conductance of the arc. To determine the value of conductance, a mathematical model consists of four sub-stages defining the transition process of the breaker from the closed state to the open state. These stages are defined as follows: closed breaker, arcing, arc extinguishing, and open stages [43], [44]. The modeling of the closed stage is implemented by using a constant resistor with a relatively small resistance value of 1 $\mu\Omega$ is used for modeling closed circuit breaker. The same concept is used for the open circuit breaker stage with a resistance value raised to a suitably high value of MΩ. The arcing stage and the extinguishing stage are modeled by using a series connection of Mayer arc model, which could be deduced as follows [13], [43]:

- An imbalance occurs between heating power resulting from the arc (P_H) and cooling power due to energy dissipated from the arc (P_o). That imbalance is translated into energy stored within the arc column $Q(t)$ as given in (1). It should be noted that the arc diameter and length affects both powers and therefore, they are included within the equation. However, the following derivation is commonly used among researchers commonly used derivation [12], [13], [16], [22], [23], [43], [44]

$$\frac{dQ(t)}{dt} = P_H - P_o \tag{1}$$

- The arc conductance $g_m(t)$ is considered a function of the stored energy $Q(t)$ as given in (2) where τ is the arc time constant.

$$g_m(t) = K\frac{Q(t)}{P_o\tau} \tag{2}$$

- The first equation in (1) could be rewritten in terms of the arc conductance as in (3).

$$\frac{dQ(t)}{dg_m}\frac{dg_m}{dt} = P_H - P_o \tag{3}$$

- By substitution (2) in (3) and considering heating power to be equal to the amount of electrical power from the arc (v $\times$i), where v is the arc voltage and i is the arc current, we get the equation in (4).

$$\frac{P_o\tau}{g_m}\frac{dg_m}{dt} = (v \times i) - P_o \tag{4}$$

- Considering that conductance $g_m = v/i$ and by rearranging equation (4), we get the final form in (5).

$$\frac{dg_m}{dt} = \frac{1}{\tau}\left(\frac{i^2}{P_o} - g_m\right) \tag{5}$$

The four sub-models form a combined contact model. Once the contact receives the open signal, each sub-model is activated at the corresponding time. It is distinctly obvious that Mayr's equation employs two variables to susceptible the characteristics of the dynamic arc. Those variables are the arc time constant (τ) and the coefficient of cooling power (P_o). The modeling of the SF6 interrupter was built using MODELS tool available on ATP/EMTP. The tool allows the acquisition of electrical measurements from the system and applying mathematical calculations in (5) using coded software within MODELS component. The SF6 interrupter model and the testing system are shown in Fig. 1.

B. MODELING OF THE COMMUTATING BRANCH

The DC CB suffers from the lack of a naturally commutating zero-current. This mandated the connection of additional elements that injects zero-current crossing during faults. This additional element is used as an L-C filter or termed the commutating parallel branch. The L-C filter injects an oscillating current during faults that superimpose the current through the breaker. Such oscillating effect allows the current through the breaker to pass through a zero-crossing point required for the interrupter to extinguish the arc. The commutating branch is modeled using L, C, and switch that are connected in parallel with the black box model [13].

C. MODELING OF THE ENERGY ABSORBING ELEMENT

A metal-oxide varistor (MOV) is also connected in parallel with the interrupter and the commutation branch. The MOV is characterized by its non-linear current-voltage characteristic allowing it to respond to overvoltage generated in power systems [13]. This element is used to store the excess energy generated from the fault incident.

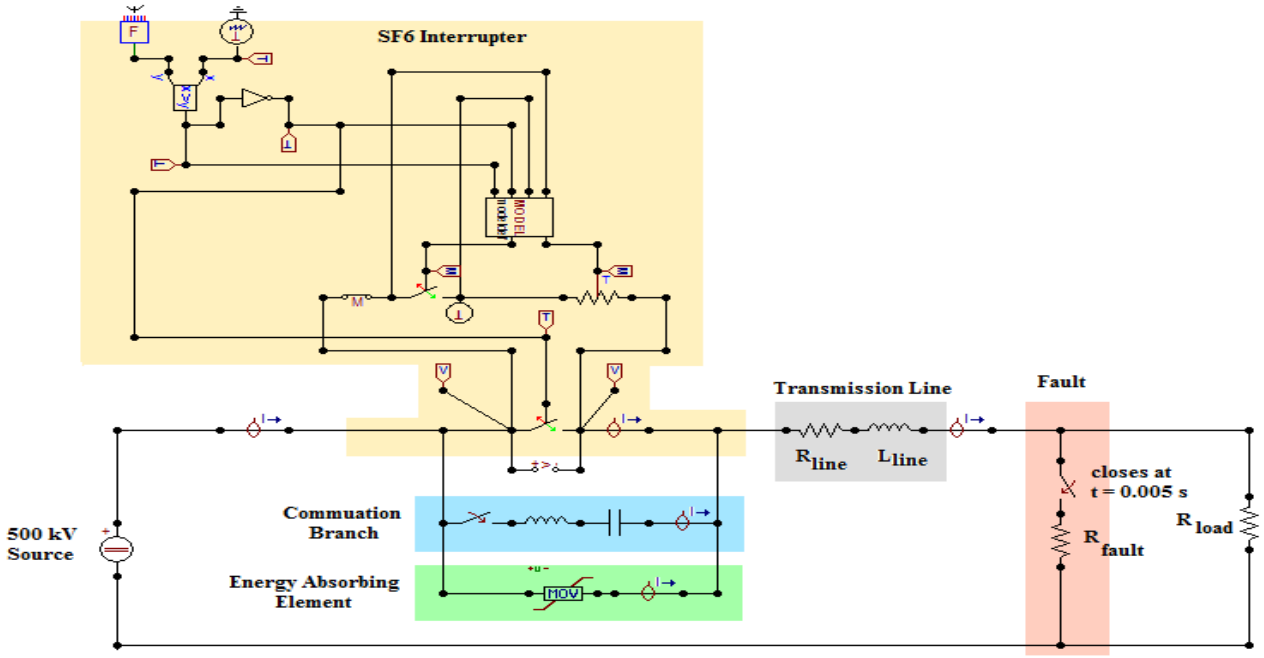

FIGURE 1. Testing system using ATP/EMTP.

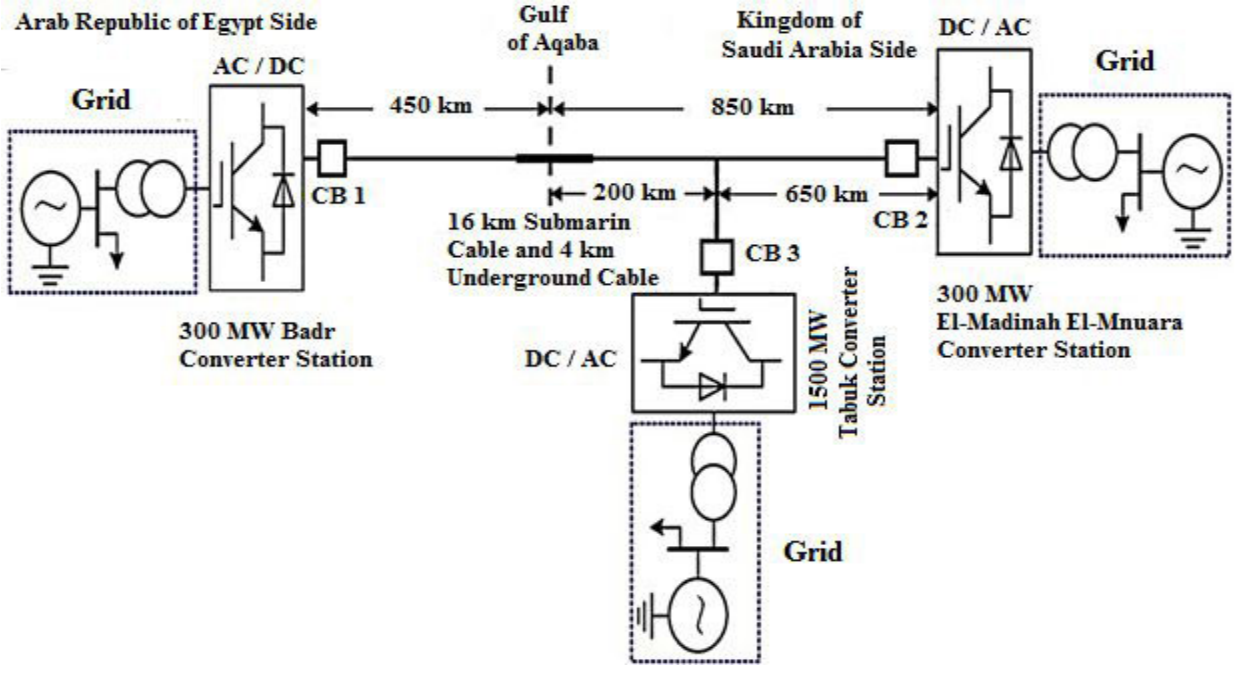

FIGURE 2. The schematic diagram of the HVDC transmission line between Egypt and the Kingdom of Saudi Arabia.

III. SIMULATION RESULTS FOR PARAMETER IMPACT UPON TRV AND RRRV

To address the main aim of the paper in investigating the impact of CB parameters on TRV and RRRV, a testing system that is based on a mega project that is currently under construction to interchange energy between Egypt and Kingdom of Saudi Arabia as presented in [16] was modeled using ATP/EMTP software. The system simulates a part of 3000 MVA, 500 kV HVDC interconnection between Egypt and the Kingdom of Saudi Arabia that is described in Fig. 2. The project consists of two 500 kV AC/DC substations in Badr City, a linking station, and a 1,300 kilometer transmission line to Medina and Tabuk in Saudia Arabia. In this paper, it is focused upon 450 km overhead DC transmission line that is located in Egypt and connects Badr substation and Elnabaq switching station. The simulated system is shown in

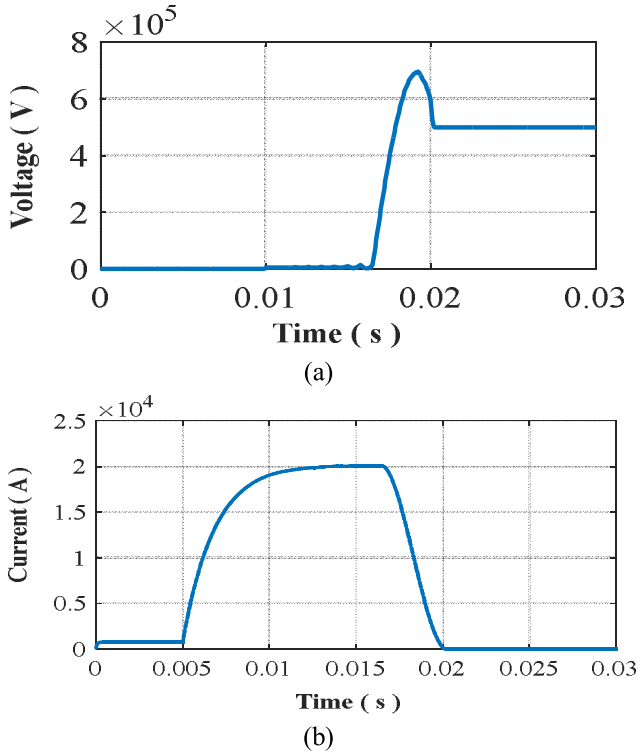

FIGURE 3. The voltage and current of the HVDC CB during the initial Case (a) Voltage across CB and (b) Current through HVDC CB.

Fig. 1 which includes a 500 kV HVDC source that is used to provide a power supply to a load of 650 Ω (R load). The source and load are connected using a 450 km DC overhead transmission line that is modeled using a resistance R_{Line} of 24.5 Ω and inductance L_{Line} of 45 mH. The HVDC CB is modeled as explained in section II with SF6 interrupter modeled using MODELS component with cooling power P_o set 85 MW and arc time constant τ set to 2 μs. The L and C of the commutation branch are set to 0.3 mH and 50 μF. The previous parameters are used only for the initial testing case and are varied one by one to investigate their effect upon the TRV and RRRV. Finally, the energy absorber element with clipping voltage of 650 kV

The initial testing case includes the initiation of a fault is initiated at 5 ms with fault resistance of 0.1 Ω at the end of the line as shown in Fig. 1. The tripping circuit responds by sending a tripping signal to the breaker at 10 ms. The resulting TRV, currents through SF6 interrupter, L-C, MOV, and DC CB are shown in Figs. 3 and 4. The analysis will be undergone through variation of the parameters of the CB and recording their impact upon the resulting TRV and RRRV. The parameters include the cooling power, arc time constant, capacitance, and inductance of the L-C filter.

A. EFFECT OF COOLING POWER

The parameters of the HVDC CB are set as follows, time constant of 10 μs, inductance, and capacitance of commutating branch L-C are 0.3 mH and 100 μF respectively.

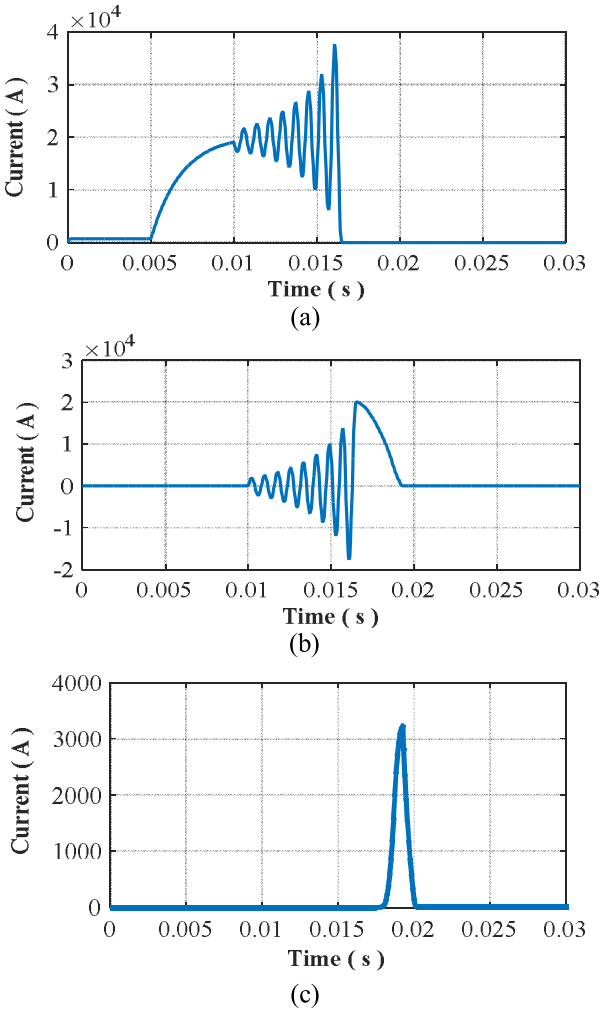

FIGURE 4. The currents of the interrupter, filter, and MOV units during the initial Case (a) Current through SF6 Interrupter, (b) Current through L-C, and (c) Current through MOV.

The fault resistance is 0.1 Ω. The cooling power is varied from 85 MW to 115 MW. The resulting voltages and fault currents from the ATP-simulation are shown in Fig. 5. The remaining waveforms within the papers are from simulation process. The results show a significant reduction in arcing time from 4.8 ms to 3.6 ms when the cooling power is increased from 85 MW to 115 MW respectively as shown in Fig. 5 (b). On the other, the peak value of the TRV following the extinguishing of the arc is relatively unchanged as shown in Fig. 5 (a). It should be noted that the waveforms of 110 MW and 115 MW are coinciding above each other in figure. The RRRV is also noticed to be identical in all cases with different cooling power. Hence, the results indicate that changing the cooling power of the gaseous interrupter has a huge impact in reducing the arcing time with little to almost no impact on the TRV and RRRV. Also, the initial current before fault in Fig. 5(b) is of non-zero value but due to the gigantic rise in fault current, the current before appears in figure to be so small and almost near-zero. To avoid this, a zoomed figure of Fig. 5(b) is shown in 5(c), which clearly shows that

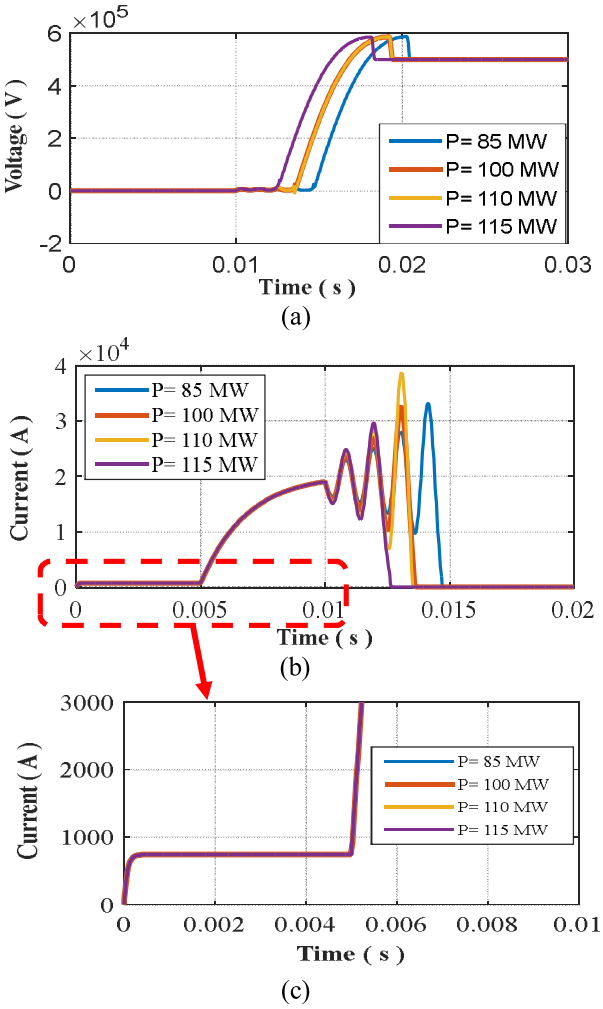

FIGURE 5. Effect of changing cooling power on (a) Voltage across CB and (b) Current through SF6 interrupter (c) Zoomed view of current in (b).

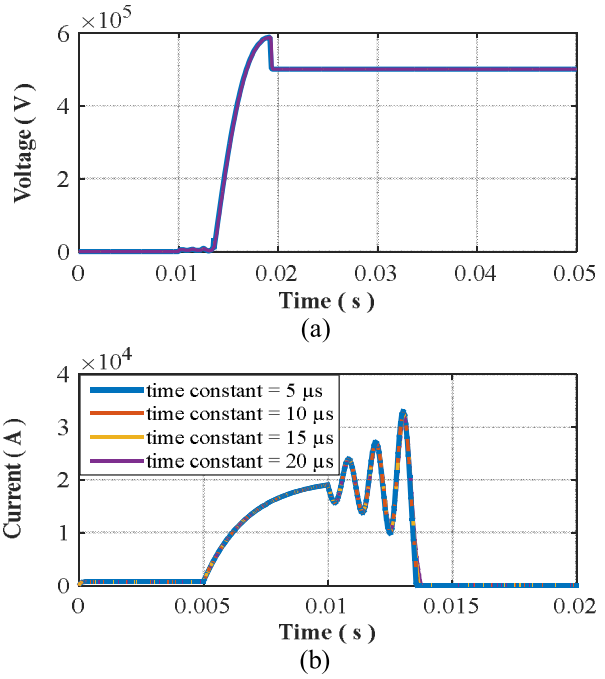

FIGURE 6. Effect of changing the time constant on (a) Voltage across CB and (b) Current through SF6 interrupter.

TABLE 2. TRV, RRRV and arcing time values for different values of L.

L (mH)	TRV (kV)	RRRV (kV/μs)	Arcing Time (ms)
0.2	586.3	1.836	2.311
0.25	586.51	1.807	2.705
0.30	587.36	1.784	3.789
0.35	587.41	1.740	4.183

current before fault is of non-zero value. This applies for the remaining figures of this study.

B. EFFECT OF CHANNGING ARCINIG TIME CONSTANT

In this case, the cooling power will be fixed to 110 MW while the remaining parameters including L, C, and fault resistance will be the same as in the previous case. The time constant is varied from 5 μs to 20 μs. The results are shown in Fig. 6. The results show that variation in time constant had negligible impact on arcing time, TRV, or RRRV.

C. EFFECT OF CHANGING THE IDUCTANCE OF THE COMMUTATION BRANCH

The time constant and cooling power of the Mayer model are fixed at 20 μs and 110 MW respectively for this case. The capacitance of the commutating branch and fault resistance are taken as in section III-A. The inductance of the commutation branch is changed from 0.2 to 0.35 mH. The arcing time, TRV, and RRRV for each inductance are presented in Table 2. The results are shown in Fig. 7. The results show that reducing the inductance value from 0.35 mH to 0.2 mH led to a reduction in arcing time from 4.183 ms to 2.311 ms. While for the TRV, the reduction is limited from 587 kV to 586 kV. The same observation is noted for RRRV. Hence, it could be concluded that the variation of inductance has a significant effect on arcing time but a negligible impact on TRV and RRRV. Such conclusion is similar to that in section III-A regarding the effect of the cooling power of the interrupter.

D. EFFECT OF CHANGING THE CAPACITANCE OF THE COMMUTATION BRANCH

In this particular case, the testing procedure is changed to combine more than one parameter varied. This change is based on the initial analysis showing that the capacitance had a significant impact on TRV, RRRV, and arcing time. That raises question of whether such impact would be affected by the value of the cooling power or the time constant or not. For this reason, the testing procedure will include varying the capacitance value from 30 μF to 200 μF for different cooling powers from 85 MW to 110 MW. In such a way, the duel effect of both capacitance and cooling power values could be analyzed. This procedure was also applied for analyzing the duel effect of the capacitance and the arcing

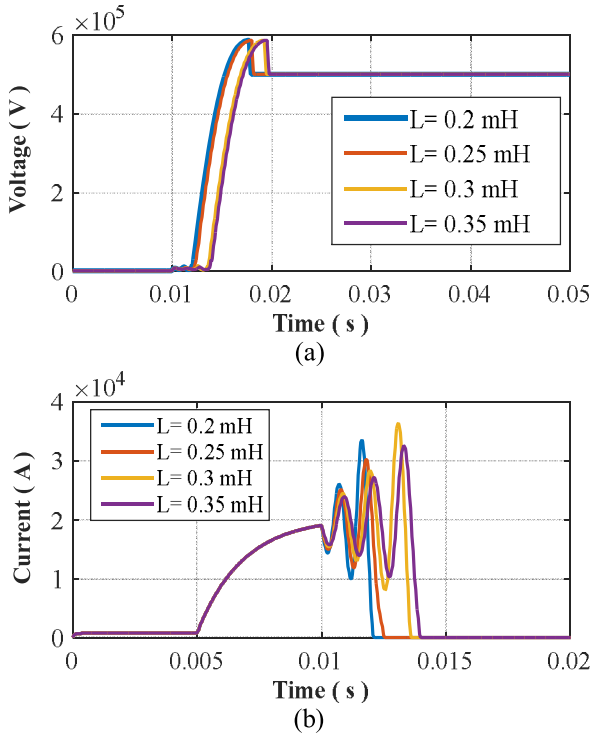

FIGURE 7. Effect of changing L on (a) Voltage across CB and (b) Current through SF6 interrupter.

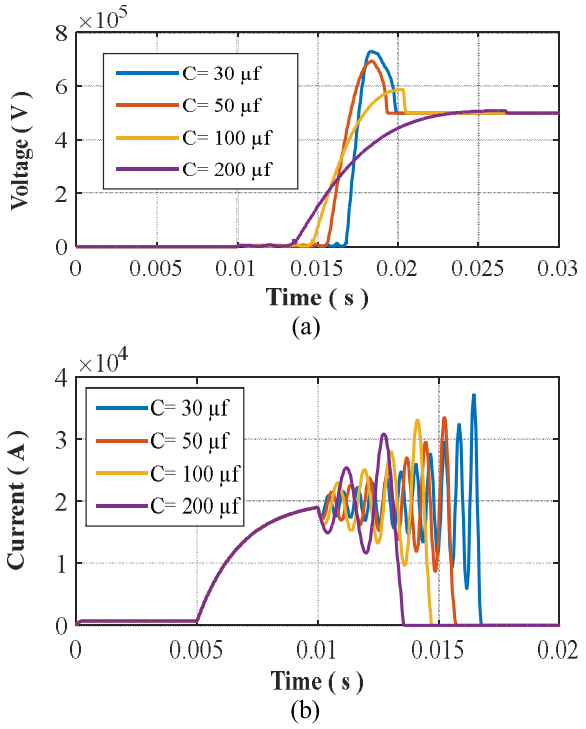

FIGURE 8. Effect of changing C with P_o = 85 MW on (a) Voltage across CB and (b) Current through SF6 interrupter.

TABLE 3. TRV, RRRV and arcing time vlaues for different values of C and P_o.

P_o (MW)	C (µF)	TRV (kV)	RRRV (kV/µs)	Arcing Time (ms)
85	30	730.73	6.259	9.983
	50	694.48	3.1486	5.817
	100	587.74	1.828	4.793
	200	508.05	0.873	3.631
100	30	730.37	5.671	5.643
	50	694.29	3.400	4.921
	100	584.08	1.635	3.687
	200	508.06	0.977	3.448
110	30	733.19	5.450	4.576
	50	693.89	3.590	4.183
	100	587.37	1.693	3.561
	200	507.89	0.786	2.114

time constant by varying the capacitance value from 30 μF to 200 μF for different time constants from 5 μs to 20 μs. The remaining parameters and fault resistance were taken as in section III-A

1) THE DUEL EFFECT OF THE CAPACITANCE AND COOLING POWER

For the study of the duel effect of the capacitance and cooling power, the time constant was set to 10 μs. The capacitance is varied from 30 μF to 200 μF with the cooling power (P_o) set to 85 MW. The same variation of capacitance values is done for cooling powers of 100 MW and 110 MW. The TRV, RRRV, and arcing time values are presented in Table 3. The results of the variation of capacitance for each cooling power are shown in Figs. 8 to 10.

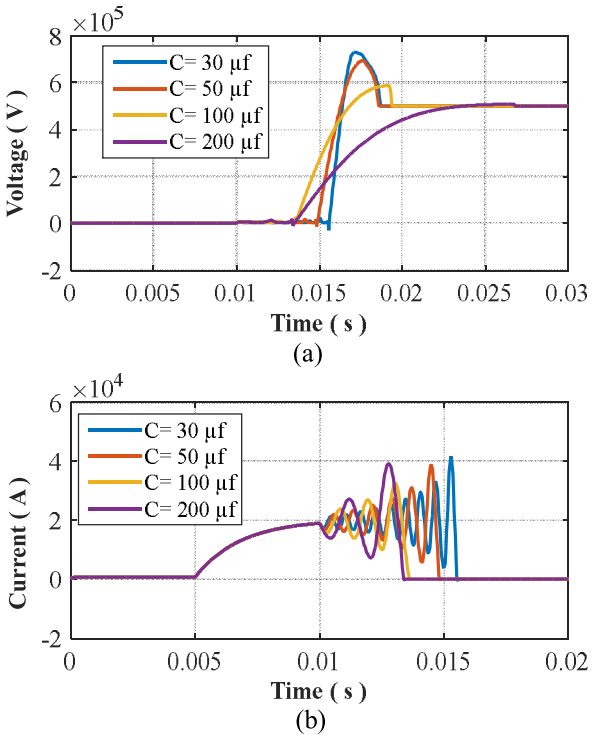

FIGURE 9. Effect of changing C with P_o = 100 MW on (a) Voltage across CB and (b) Current through SF6 interrupter.

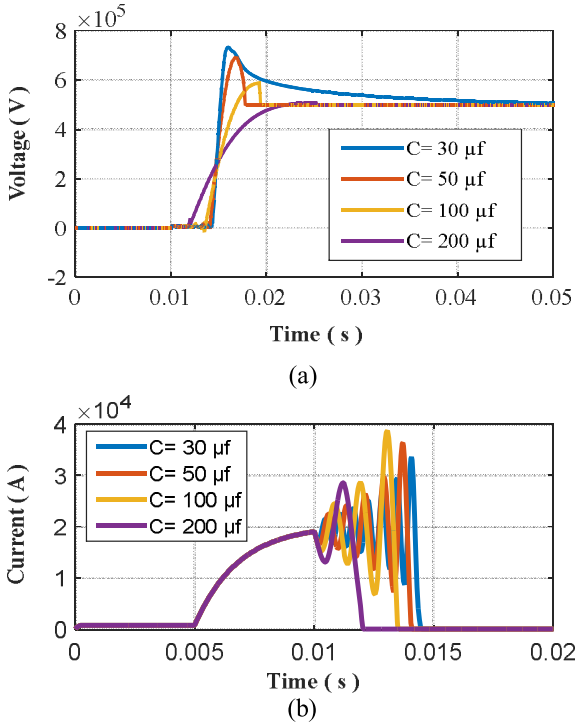

FIGURE 10. Effect of changing C with $P_o = 110$ MW on (a) Voltage across CB and (b) Current through SF6 interrupter.

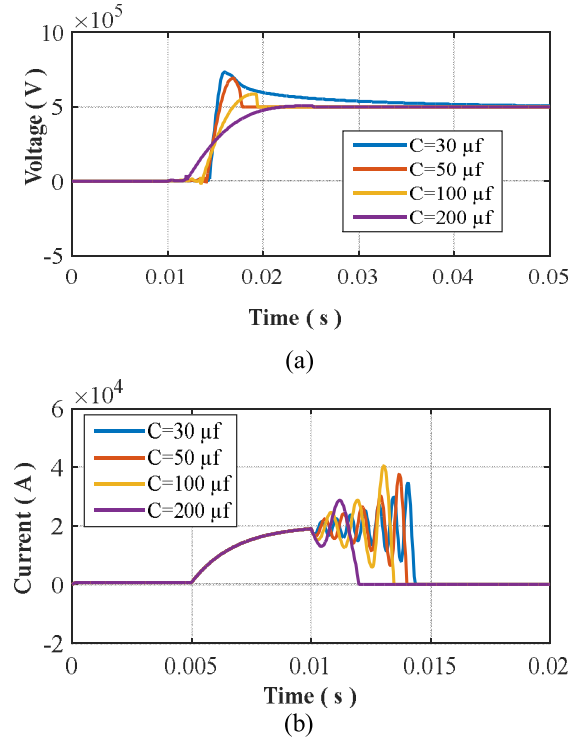

FIGURE 11. Effect of changing C with $\tau = 5$ μs on (a) Voltage across CB and (b) Current through SF6 interrupter.

2) THE DUEL EFFECT OF THE CAPACITANCE AND ARC TIME CONSTANT

The same sequence of testing is undergone for studying the duel effect of the capacitance and time constant on the TRV, RRRV, and arcing time. The cooling power was set to 110 MW. The capacitance is varied from 30 μF to 200 μF with the time constant (τ) set to 5 μs. The same variation of capacitance values is done for time constants of 10, 15, and 20 μs. The TRV, RRRV, and arcing time values are presented in Table 4. The results of the variation of capacitance for each time constant are shown in Figs. 11 to 14.

TABLE 4. TRV, RRRV and arcing time values for different values of C and τ.

τ (µs)	C (µF)	TRV (kV)	RRRV (kV/µs)	Arcing Time (ms)
5	30	733.09	6.053	4.412
	50	693.90	3.750	4.058
	100	587.40	1.774	3.528
	200	507.94	0.896	2.016
10	30	733.03	5.450	4.576
	50	693.89	3.590	4.183
	100	587.37	1.693	3.561
	200	507.89	0.786	2.114
15	30	733.16	6.367	5.172
	50	693.87	3.655	4.297
	100	587.37	1.793	3.700
	200	505.99	0.804	2.241
20	30	733.27	6.239	5.351
	50	693.75	3.655	4.456
	100	587.36	1.793	3.815
	200	507.94	0.804	2.370

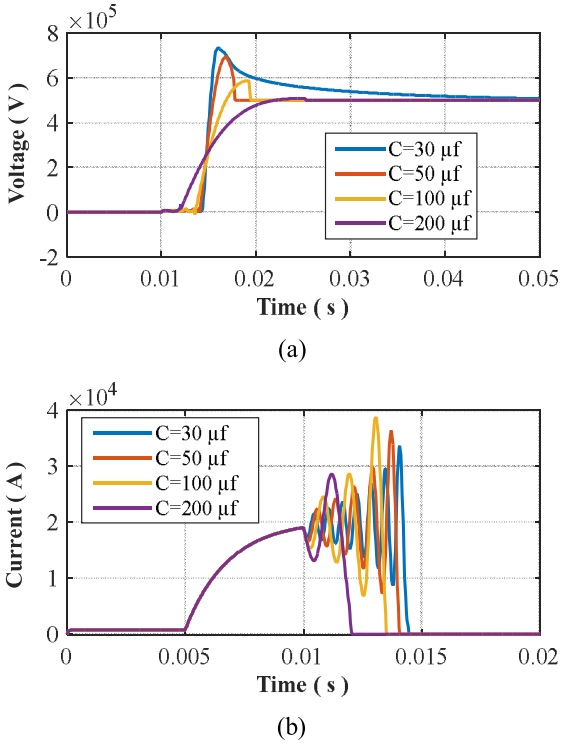

FIGURE 12. Effect of changing C with $\tau = 10$ μs on (a) Voltage across CB and (b) Current through SF6 interrupter.

E. EFFECT OF THE FAULT RESISTANCE

The impact of the fault resistance upon the TRV and RRRV was examined by varying the resistance from 0.1 Ω to 10 Ω.

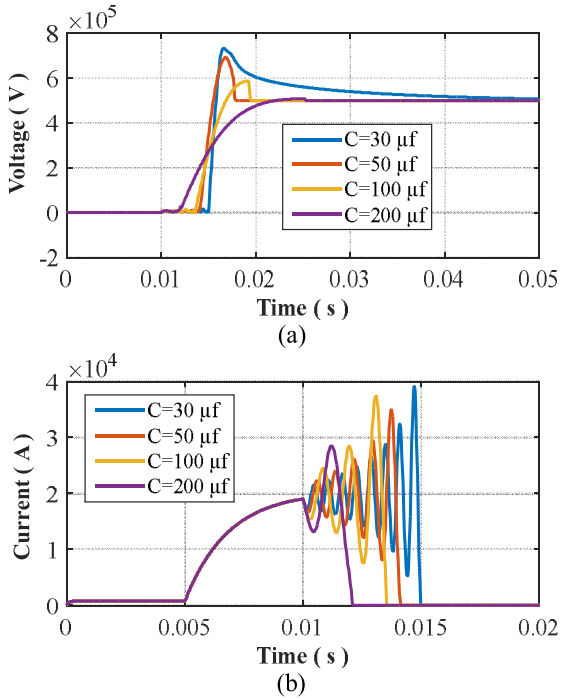

FIGURE 13. Effect of changing C with $\tau = 15\ \mu s$ on (a) Voltage across CB and (b) Current through SF6 interrupter.

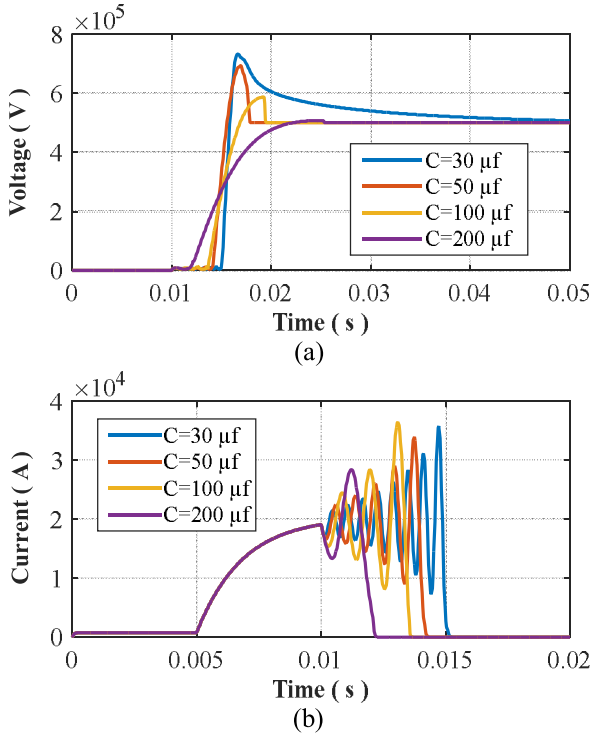

FIGURE 14. Effect of changing C with $\tau = 20\ \mu s$ on (a) Voltage across CB and (b) Current through SF6 interrupter.

The cooling power and time constant of the Mayr model were set to 110 MW and 20 μs respectively. The L and C of the commutation circuit were set to 0.3 mH and 100 μF respectively. The results are presented in Table 5 and shown in Fig. 15.

TABLE 5. TRV, RRRV, and arcing time values for different values of R.

R (Ω)	TRV (kV)	RRRV (kV/µs)	Arcing Time (ms)
0.1	587.35	1.8314	3.789
1	576.27	1.773	3.757
4	545.13	1.559	2.672
10	509.48	1.280	1.606

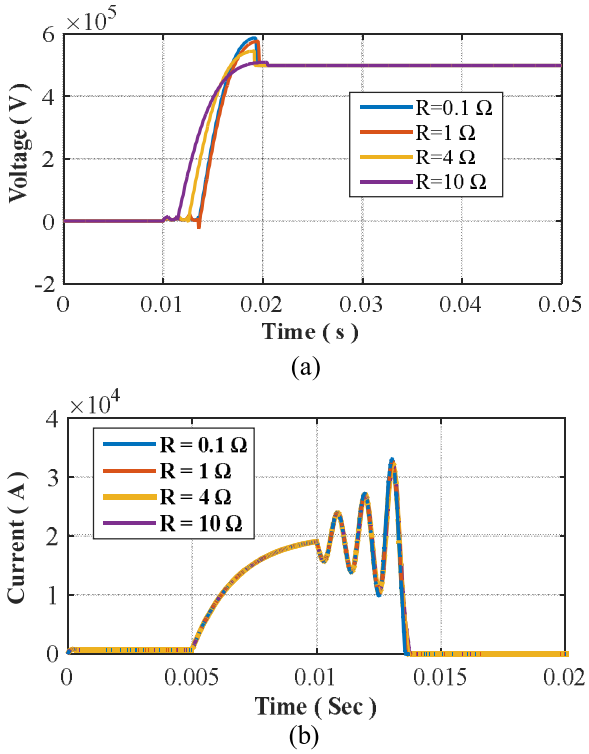

FIGURE 15. Effect of changing fault resistance on (a) Voltage across CB and (b) Current through SF6 interrupter.

IV. ANALYSIS OF THE PARAMETERS IMPACT ON TRV AND RRRV

The presented previous results showed that the parameters of CB had a different level of impact upon TRV, RRRV, and arcing time. From the arcing time point of view, the cooling power, inductance, and capacitance had a significant impact in reducing the arcing time. While for TRV and RRRV, the arcing time constant, cooling power, and inductance of the commutation branch had negligible impact. Only the capacitance had a direct impact upon TRV and RRRV. The combined effect of capacitance and cooling power or time constant didn't change the level of the impact of the capacitance upon TRV and RRRV. Hence, it could be concluded that to reduce the TRV and RRRV, the main parameter that designers should consider is the capacitance of the commutation circuit.

V. CONCLUSION

DC circuit breakers had been under increased investigation by researchers for their vital role in HVDC networks. The design of HVDC CB included a gaseous interrupter, L-C commutation branch, and MOV. The analysis of the effect

of the parameters of the HVDC CBs was mainly focused upon the arcing time. In this paper, the effect of different parameters was simulated and analyzed. The system simulates a part of 3000 MVA, 500 kV HVDC interconnection between Egypt and the Kingdom of Saudi Arabia. The CB and testing circuit were simulated using ATP/EMTP software package. The parameters considered were the cooling power, time constant of Mayr model, L, and C. For the study of the impact of each parameter, the remaining parameters were kept constant.

The results showed that the cooling power, inductance, and capacitance had a significant impact in reducing the arcing time. However, only the capacitance had the capability of reducing the TRV and RRRV. In this context, the main parameter that should be considered to reduce TRV within acceptable ranges will be the capacitance of the L-C filter. This conclusion is highly important to be considered by designers of HVDC CBs to reach a safe opening of the breaker and avoid failures due to TRVs.

ACKNOWLEDGMENT

The authors extend their appreciation to the Deputyship for Research & Innovation, Ministry of Education in Saudi Arabia for funding this research work through the project number 223202.

REFERENCES

[1] H. Zhou, W. Yao, X. Ai, D. Li, J. Wen, and C. Li, "Comprehensive review of commutation failure in HVDC transmission systems," *Electr. Power Syst. Res.*, vol. 205, Apr. 2022, Art. no. 107768.

[2] Y. Tang, F. Li, Q. Wang, B. Chen, Y.-L. Jiang, and X.-J. Guo, "Power stability analysis of UHVDC systems hierarchically connected to AC systems," *Electr. Power Syst. Res.*, vol. 163, pp. 715–724, Oct. 2018.

[3] Y. Xiong, W. Yao, J. Wen, S. Lin, X. Ai, J. Fang, J. Wen, and S. Cheng, "Two-level combined control scheme of VSC-MTDC integrated offshore wind farms for onshore system frequency support," *IEEE Trans. Power Syst.*, vol. 36, no. 1, pp. 781–792, Jan. 2021.

[4] X. Liang and M. Abbasipour, "HVDC transmission and its potential application in remote communities: Current practice and future trend," *IEEE Trans. Ind. Appl.*, vol. 58, no. 2, pp. 1706–1719, Mar. 2022.

[5] M. Muniappan, "A comprehensive review of DC fault protection methods in HVDC transmission systems," *Protection Control Mod. Power Syst.*, vol. 6, no. 1, pp. 1–20, Jan. 2021.

[6] Y. Li, Z. Zhang, C. Rehtanz, L. Luo, S. Rüberg, and F. Liu, "Study on steady- and transient-state characteristics of a new HVDC transmission system based on an inductive filtering method," *IEEE Trans. Power Electron.*, vol. 26, no. 7, pp. 1976–1986, Jul. 2011.

[7] F. Mohammadi, K. Rouzbehi, M. Hajian, K. Niayesh, G. B. Gharehpetian, H. Saad, M. H. Ali, and V. K. Sood, "HVDC circuit breakers: A comprehensive review," *IEEE Trans. Power Electron.*, vol. 36, no. 12, pp. 13726–13739, Dec. 2021.

[8] A. Raza, A. Mustafa, U. Alqasemi, K. Rouzbehi, R. Muzzammel, S. Guobing, and G. Abbas, "HVdc circuit breakers: Prospects and challenges," *Appl. Sci.*, vol. 11, no. 11, p. 5047, May 2021.

[9] M. J. Pérez-Molina, D. M. Larruskain, P. Eguía López, and G. Buigues, "Challenges for protection of future HVDC grids," *Frontiers Energy Res.*, vol. 8, p. 33, Feb. 2020.

[10] H.-W. Choi, I.-S. Jeong, and H.-S. Choi, "Stability improvement of DC power system according to applied DC circuit breaker combined with fault current limitation characteristics of superconductivity," *IEEE Trans. Appl. Supercond.*, vol. 28, no. 7, pp. 1–4, Oct. 2018.

[11] X. Zhang, J. Bai, G. Cao, and C. Chen, "Optimizing HVDC control parameters in multi-infeed HVDC system based on electromagnetic transient analysis," *Int. J. Electr. Power Energy Syst.*, vol. 49, pp. 449–454, Jul. 2013.

[12] O. E. Gouda, M. I. Awaad, and Z. E. Afifi, "Impact of superconducting current limiter on the gaseous HVDC circuit breakers characteristics," *Electr. Power Syst. Res.*, vol. 199, Oct. 2021, Art. no. 107442.

[13] O. E. Gouda, G. Amer, M. Awaad, and M. Ahmed, "Cascaded HVDC gaseous circuit breaker performance using black box arc model," *Electr. Eng.*, vol. 103, no. 2, pp. 1199–1215, Apr. 2021.

[14] Y. Wu, Y. Wu, M. Rong, and F. Yang, "Development of a novel HVdc circuit breaker combining liquid metal load commutation switch and two-stage commutation circuit," *IEEE Trans. Ind. Electron.*, vol. 66, no. 8, pp. 6055–6064, Aug. 2019.

[15] W. Sima, Z. Fu, M. Yang, T. Yuan, P. Sun, X. Han, and Y. Si, "A novel active mechanical HVDC breaker with consecutive interruption capability for fault clearances in MMC-HVDC systems," *IEEE Trans. Ind. Electron.*, vol. 66, no. 9, pp. 6979–6989, Sep. 2019.

[16] O. E. Gouda, D. K. Ibrahim, and A. Soliman, "Parameters affecting the arcing time of HVDC circuit breakers using black box arc model," *IET Gener. Transmiss. Distrib.*, vol. 13, no. 4, pp. 461–467, Feb. 2019.

[17] B. Xiang, L. Zhang, K. Yang, Y. Tan, Z. Liu, Y. Geng, J. Wang, and S. Yanabu, "Arcing time of a DC circuit breaker based on a superconducting current-limiting technology," *IEEE Trans. Appl. Supercond.*, vol. 26, no. 7, pp. 1–5, Oct. 2016.

[18] T. Qin, E. Dong, G. Liu, and J. Zou, "Recovery of dielectric strength after DC interruption in vacuum," *IEEE Trans. Dielectr. Electr. Insul.*, vol. 23, no. 1, pp. 29–34, Feb. 2016.

[19] M. K. Bucher and C. M. Franck, "Fault current interruption in multiterminal HVDC networks," *IEEE Trans. Power Del.*, vol. 31, no. 1, pp. 87–95, Feb. 2016.

[20] D. Jovcic, G. Tang, and H. Pang, "Adopting circuit breakers for high-voltage DC networks: Appropriating the vast advantages of DC transmission grids," *IEEE Power Energy Mag.*, vol. 17, no. 3, pp. 82–93, May 2019.

[21] K. Zhu, X. Li, S. Jia, W. Zhang, and W. Gao, "Study of the switching arc characteristics of a 500 kV HVDC self-excited oscillatory metallic return transfer breaker," *IEEE Trans. Dielectr. Electr. Insul.*, vol. 22, no. 1, pp. 128–134, Feb. 2015.

[22] H. Nakao, Y. Nakagoshi, M. Hatano, T. Koshizuka, S. Nishiwaki, A. Kobayashi, T. Murao, and S. Yanabu, "DC current interruption in HVDC SF_6 gas MRTB by means of self-excited oscillation superimposition," *IEEE Trans. Power Del.*, vol. 16, no. 4, pp. 687–693, Oct. 2001.

[23] T. Ohtaka, V. Kertész, and R. Peter Paul Smeets, "Novel black-box arc model validated by high-voltage circuit breaker testing," *IEEE Trans. Power Del.*, vol. 33, no. 4, pp. 1835–1844, Aug. 2018.

[24] F. Bizzarri, A. Brambilla, G. Gruosso, G. S. Gajani, M. Bonaconsa, and F. Viaro, "A new black-box model of SF6 breaker for medium voltage applications," in *Proc. 43rd Annu. Conf. IEEE Ind. Electron. Soc.*, Beijing, China, Oct. 2017, pp. 32–37, doi: 10.1109/IECON.2017.8216010.

[25] M. Walter and C. Franck, "Improved method for direct black-box arc parameter determination and model validation," *IEEE Trans. Power Del.*, vol. 29, no. 2, pp. 580–588, Apr. 2014.

[26] R. D. Garzon, *High Voltage Circuit Breakers: Design and Applications*, 2 ed. New York, NY, USA: Marcel Dekker Inc, 2002.

[27] J.-G. Lee, U. A. Khan, H.-Y. Lee, and B.-W. Lee, "Impact of SFCL on the four types of HVDC circuit breakers by simulation," *IEEE Trans. Appl. Supercond.*, vol. 26, no. 4, pp. 1–6, Jun. 2016.

[28] H. Xiao, X. Huang, F. Xu, L. Dai, Y. Zhang, Z. Cai, and Y. Liu, "Improved multiline HVDC circuit breakers with asymmetric conducting branches," *Int. J. Electr. Power Energy Syst.*, vol. 137, May 2022, Art. no. 107882.

[29] M. Ahmad, Z. Wang, M. Shafique, and M. H. Nadeem, "Significance of fault-current-limiters and parameters optimization in HVDC circuit breakers for increased capacity of VSC-HVDC transmission networks application," *Energy Rep.*, vol. 8, pp. 878–892, Nov. 2022.

[30] J. Yu, Z. Xu, Z. Zhang, and Y. Song, "Hybrid HVDC circuit breakers with an energy absorption branch of a parallel arrester structure," *High Voltage*, vol. 7, no. 1, pp. 197–207, Feb. 2022.

[31] H. Xiao, B. Liu, X. Huang, Z. Cai, and Y. Zhang, "Topology and control of a novel hybrid HVDC circuit breaker with self-powered capability," *Energy Rep.*, vol. 8, pp. 1165–1173, Aug. 2022.

[32] M. Zhou, W. Xiang, W. Zuo, W. Lin, and J. Wen, "A novel HVDC circuit breaker for HVDC application," *Int. J. Electr. Power Energy Syst.*, vol. 109, pp. 685–695, Jul. 2019.

[33] E. A. Awad, E. A. Badran, and F. H. Youssef, "Mitigation of switching overvoltages in microgrids based on SVC and supercapacitor," *IET Gener. Transmiss. Distrib.*, vol. 12, no. 2, pp. 355–362, Jan. 2018.

[34] N. Kularatna, J. Fernando, A. Pandey, and S. James, "Surge capability testing of supercapacitor families using a lightning surge simulator," *IEEE Trans. Ind. Electron.*, vol. 58, no. 10, pp. 4942–4949, Oct. 2011.
[35] N. Kularatna, J. Fernando, and A. Pandey, "Surge endurance capability testing of supercapacitor families," in *Proc. 36th Annu. Conf. IEEE Ind. Electron. Soc.*, Nov. 2010, pp. 1858–1863.
[36] Y. He, Q. Yang, Y. Li, S. Kim, F. Z. Peng, M. Bosworth, L. Wang, Z. Jin, Y. Shi, N. Bonaventura, M. Steurer, C. Xu, and L. Graber, "Control development and fault current commutation test for the Edison hybrid circuit breaker," *IEEE Trans. Power Electron.*, vol. 38, no. 7, pp. 8851–8865, Jul. 2023
[37] X. Zhang, C. Zhuo, and X. Yang, "A natural commutation current topology of hybrid HVDC circuit breaker integrated with limiting fault current," *IET Gener. Transmiss. Distrib.*, vol. 17, no. 7, pp. 1509–1524, Apr. 2023.
[38] G. A. Ludin, H. Zeerak, Q. Tayyab, A. S. Irshad, H. Matayoshi, N. Prabaharan, A. Rasooli, and T. Senjyu, "Novel hybrid fault current limiter with hybrid resonant breaker in multi-terminal HVDC transmission system," *Electr. Power Syst. Res.*, vol. 221, Aug. 2023, Art. no. 109403.
[39] M. Roshani Diz and B. Vahidi, "Integration of E-core DC reactor based on thyristors with hybrid HVDC breaker," *Electr. Power Syst. Res.*, vol. 224, Nov. 2023, Art. no. 109777.
[40] T. E. Browne, "Practical modeling of the circuit breaker ARC as a short line fault interrupter," *IEEE Trans. Power App. Syst.*, vol. PAS-97, no. 3, pp. 838–847, May 1978.
[41] A. Islam, D. Birtwhistle, and T. K. Saha, "Simulation of the thermal current interruption process of air-break interrupters for future mv application," *Electr. Power Syst. Res.*, vol. 182, May 2020, Art. no. 106264.
[42] V. V. Popovtsev, A. I. Khalyasmaa, and Y. V. Patrakov, "Fluid dynamics calculation in SF6 circuit breaker during breaking as a prerequisite for the digital twin creation," *Axioms*, vol. 12, no. 7, p. 623, Jun. 2023.
[43] E. A. Badran, M. A. Abd-Allah, A. H. Hamza, and T. Elyan, "A proposed transient recovery voltage mitigation technique for generator-circuit-breaker fed faults," *J. Electr. Syst.*, vol. 9, no. 1, pp. 66–72, 2013.
[44] G. Bizak, P. Zunko, and D. Povh, "Combined model of SF6 circuit breaker for use in digital simulation programs," *Trans. Power Del.*, vol. 19, no. 1, pp. 174–180, 2004.

TAMER ELIYAN was born in Qalyubia, Egypt, in September 1983. He received the B.Sc. degree (Hons.) in electrical power and machines and the M.Sc. and Ph.D. degrees in high-voltage engineering from the Electrical Power and Machines Department, Faculty of Engineering at Shoubra, Benha University, Cairo, Egypt, in 2005, 2010, and 2014, respectively. He is currently an Associate Professor with the Electrical Engineering Department, Faculty of Engineering at Shoubra, Benha University. His research interests include transient phenomena in power networks and power systems, renewable energy, high-voltage materials engineering, high-voltage circuit breakers, and smart grids.

MAHMOUD ELSISI (Senior Member, IEEE) received the B.Sc., M.Sc., and Ph.D. degrees from the Electrical Engineering Department, Faculty of Engineering at Shoubra, Benha University, Cairo, Egypt, in 2011, 2014, and 2017, respectively.

He was an Assistant Professor with the Electrical Engineering Department, Faculty of Engineering at Shoubra, Benha University. From August 2019 to July 2022, he was an Assistant Professor with the Industry 4.0 Implementation Center and the Center for Cyber-Physical System Innovation, National Taiwan University of Science and Technology, Taipei, Taiwan. He is currently an Associate Professor with the Electrical Engineering Department, National Kaohsiung University of Science and Technology, Kaohsiung, Taiwan. His research interests include studying the machine learning, deep learning, the Internet of Things (IoT), cybersecurity, model predictive control, neural networks, fuzzy logic, Kalman filter, observers, decentralized control of largescale systems, robotic control, autonomous vehicle control, renewable energy, power system dynamics, stability and control, nuclear power plant control, wind energy conversion systems, faults diagnosis, and power transformers.

MAMDOUH L. ALGHAYTHI (Member, IEEE) received the B.S. degree from Al Jouf University, Sakakah, Saudi Arabia, in 2012, the M.S. degree from Southern Illinois University, Carbondale, IL, USA, in 2015, and the Ph.D. degree from the University of Missouri, Columbia, MO, USA, in 2020, all in electrical engineering. He is currently an Assistant Professor with the Department of Electrical Engineering, Jouf University, where he is also the Chair of the Electrical Engineering Department and the Coordinator of the Master's Program in Renewable Energy. He has authored or coauthored many journal articles and conference papers. His current research interests include the design and modeling of power electronics converters, renewable energy systems, reliability aspects of dc-dc converters, smart grids, energy management, and microgrids. He is a member of the IEEE Power Electronics Society.

MESHARI S. ALSHAMMARI received the B.Sc. degree in electrical engineering from the University of Ha'il, Saudi Arabia, in 2014, and the M.E. degree in energy systems engineering and the Ph.D. degree in electrical and electronics engineering from the University of Galway, in 2017 and 2022, respectively. He is an Assistant Professor with the Electrical Engineering Department, Jouf University, Sakaka, Saudi Arabia. His research interests include the analysis of ac and dc distribution systems, dc/ac power converters for utility grid and renewable energy applications, and renewable energy integration systems. In addition, he received the Best Poster at the 7th NUI Galway Research Day, in 2017; and the Best Paper at ICRERA 2021.

FADY WADIE received the B.Sc. degree in electrical power engineering from Ain Shams University, in 2009, and the M.Sc. and Ph.D. degrees in high-voltage engineering from Benha University (Shoubra Branch), Cairo, in 2015 and 2019, respectively. He is currently a Lecturer with Egyptian Russian University. His research interests include switching transients of circuit breakers and their mitigation, wide area back-up protection, and fault detection algorithms based on communication assisted techniques.